

Anisotropic Elastoplastic Bounding Surface Model for Cohesive Soils

Hoe I. Ling, M.ASCE¹; Dongyi Yue²; Victor N. Kaliakin, M.ASCE³; and Nickolas J. Themelis⁴

Abstract: The initial stresses existing in the natural ground are anisotropic in the sense that the vertical stress is typically larger than the lateral stresses. The construction activities, such as embankments and excavation, induce anisotropy in the stress system. The stress-deformation behavior and excess pore water pressure response of soils are affected by the inherent and induced stress anisotropy. This paper presents an improved soil model based on the anisotropic critical state theory and bounding surface plasticity. The anisotropic critical state theory of Dafalias was extended into three-dimensional stress space. In addition to the isotropic hardening rule, rotational and distortional hardening rules were incorporated into the bounding surface formulation with an associated flow rule. The projection center that is used to map the actual stress point to the imaginary stress point was specified along the K_0 line instead of the hydrostatic line or at the origin of the stress space. A simplified form of plastic modulus was used and the proposed model requires a total of 12 material parameters, the same number as that of the single-ellipse time-independent version of the Kaliakin–Dafalias model. The model was validated against the undrained isotropic and anisotropic triaxial test results under compression and extension shearing modes for Kaolin Clay, San Francisco Bay Mud, and Boston Blue Clay. The effects of stress anisotropy and overconsolidation were well captured by the model. The time effect was not included in the formulations presented in this paper.

DOI: 10.1061/(ASCE)0733-9399(2002)128:7(748)

CE Database keywords: Elastoplasticity; Cohesive soils; Anisotropy; Models; Triaxial tests.

Introduction

Cam-clay models, which are based on the critical state theory, have been developed to express the elastoplastic behavior of clay (Roscoe and Burland, 1968; Schofield and Wroth 1968). They were formulated in the triaxial (p – q) space using the well-known e – $\ln p$ relationships (where p , q , and e =mean effective stress, deviator stress, and void ratio, respectively). In the original Cam-clay model (Schofield and Wroth 1968), the yield surface is bullet-shaped whereas in the modified Cam-clay model (Roscoe and Burland 1968), it is described by an ellipse. In both models, the yield surface is aligned along the p axis and hardens isotropically according to the linear e – $\ln p$ relationships following an associated flow rule. The cap model (DiMaggio and Sandler 1971; Sandler et al. 1976) was formulated in three-dimensional stress space and has a curved failure envelope. It shows improvements over the Cam-clay model as well as the elastoplastic theory

put forward by Drucker and Prager (1952) and Drucker et al. (1957). The plastic volumetric strain was used as a hardening parameter in the cap model.

A significant development in constitutive modeling was achieved when Dafalias applied his bounding surface concept to soils (Dafalias and Herrmann 1982; Dafalias 1986). Instead of a classical yield surface, a bounding surface is defined in this model so that the actual stress is mapped to the imaginary stress on the bounding surface. The distance between the real and imaginary stress is used to specify the plastic modulus of the actual stress states in terms of bounding plastic modulus. The bounding surface theory allows a smooth transition of stress in an elastic state, within and on the bounding surface. The model is very relevant for simulating the behavior of overconsolidated cohesive soils. The isotropic, anisotropic, and time-dependent versions of the bounding surface model have been proposed (e.g., Dafalias and Herrmann 1982; Anandarajah and Dafalias 1985, 1986; Dafalias and Herrmann 1986; Kaliakin and Dafalias 1990). The mathematical aspect of bounding surface theory is given in a subsequent section.

Soil exhibits anisotropic properties that may be inherent due to the fabric structure (structural anisotropy) and initial stress conditions (inherent anisotropy) or induced as a result of stress change (stress-induced anisotropy). Inherent structural anisotropy (e.g., Anandarajah et al. 1996) exists in the fabric structure where the long axis of the soil particles tends to align in a preferred horizontal direction during deposition. In clay, two types of variation of strength based on inclination of the major principal stress or deposition plane have been reported: (1) the strength is largest for vertical inclination but it reduces as the plane rotates and becomes the smallest for horizontal plane (e.g., Lo 1965); and (2) a lower strength for inclined plane compared to vertical and horizontally planes (e.g., Duncan and Seed 1966). Anisotropy of the

¹Associate Professor, Dept. of Civil Engineering and Engineering Mechanics, Columbia Univ., 500 West 120th St., New York, NY 10027. E-mail: ling@civil.columbia.edu

²Graduate Research Assistant, Dept. of Earth and Environmental Engineering, Columbia Univ., 500 West 120th St., New York, NY 10027.

³Associate Professor, Dept. of Civil and Environmental Engineering, Univ. of Delaware, Newark, DE 19716.

⁴Stanley-Thompson Professor, Dept. of Earth and Environmental Engineering, Columbia Univ., 500 West 120th St., New York, NY 10027.

Note. Associate Editor: A. Rajah Anandarajah. Discussion open until December 1, 2002. Separate discussions must be submitted for individual papers. To extend the closing date by one month, a written request must be filed with the ASCE Managing Editor. The manuscript for this paper was submitted for review and possible publication on March 22, 2001; approved on January 7, 2002. This paper is part of the *Journal of Engineering Mechanics*, Vol. 128, No. 7, July 1, 2002. ©ASCE, ISSN 0733-9399/2002/7-748–758/\$8.00+\$0.50 per page.

Table 1. Anisotropic Elastoplastic Model for Clays

| Reference | Model | Yield function/bounding surface | Hardening rule | Flow rule | Plasticity theory |
|---------------------------------------|--|--|--------------------------------------|---------------|-------------------|
| Schofield and Wroth (1968) | Original Cam-clay | $M \ln \frac{p}{p_0} + \frac{q}{p} = 0$ | Isotropic | Associated | Classical |
| Roscoe and Burland (1968) | Modified Cam-clay | $p(p - p_0) + \frac{q^2}{M^2} = 0$ | Isotropic | Associated | Classical |
| Sekiguchi and Ohta (1977) | Ohta's model (equivalent shear stress) | $M \ln \frac{p}{p_0} + \sqrt{\frac{3}{2} \left(\frac{s_{ij}}{p} - \frac{s_{ij}^0}{p_0} \right)^2} = 0$ | Isotropic | Associated | Classical |
| Anandarajah and Dafalias (1985, 1986) | Induced invariant | $(I^a - I_0^a) \left(I^a + \frac{R-2}{R} I_0^a \right) + (R-1)^2 \frac{(J^a)^2}{N^2(\theta^a)} = 0$ | Isotropic, anisotropic, distortional | Associated | Bounding surface |
| Banerjee and Yousif (1986) | Experimentally based | $\frac{3}{2M^2} \left(s_{ij}^a s_{ij}^a - \frac{1}{9} \frac{p}{p_0} s_{ij}^0 s_{ij}^0 \right) - p(p_0 - p) = 0$ | Isotropic, anisotropic | Associated | Bounding surface |
| Dafalias (1987) | Anisotropic critical state theory | $p(p - p_0) + \frac{(q - p\alpha)^2}{M^2 - \alpha^2} = 0$ | Isotropic, anisotropic | Associated | Classical |
| Crouch and Wolf (1992) | Unified model | $(\bar{I} - I_0) \left(\bar{I} + \frac{R-2}{R} I_0 \right) + (R-1)^2 \frac{(\bar{J})^2}{N^2} = 0$ | Isotropic | Nonassociated | Bounding surface |
| Whittle (1993) | MIT-E3 (equivalent shear stress) | $(s_{ij} - p\alpha_{ij})(s_{ij} - p\alpha_{ij}) - c^2 p(p_0 - p) = 0$ | Isotropic, anisotropic | Nonassociated | Bounding surface |

stress system can be related to the *in situ* stress conditions and/or stress induced by subsequent shearing (e.g., Ladd et al. 1977). K_0 conditions prevail in the natural ground where vertical overburden stress is typically larger than horizontal stress. It has to be mentioned that even for a homogeneous and structurally isotropic soil, shearing may induce anisotropic behavior in the stress-deformation relationships. Experimental results have shown that the yield surface for anisotropically consolidated clay tends to align along the K_0 line (e.g., Graham et al. 1983). The pore water pressure as well as the stress-strain response of an anisotropically consolidated clay specimen under undrained shearing were significantly affected by the initial stress ratio (Ladd and Varallyay 1965; Stipho 1978).

The critical state and cap models are, however, valid for isotropic stress conditions and for normally to lightly overconsolidated clays, involving mainly monotonic loading. There have been several attempts to model anisotropic soil behavior by extending the critical state soil models, as summarized in Table I. A brief account of these modeling approaches is given below.

An anisotropic model for normally consolidated clay was proposed by Ohta and Hata (1971). The yield surface degenerates to the original Cam-clay model for isotropic conditions. In Ohta's models (Ohta and Hata 1971; Sekiguchi and Ohta 1977), the parameter q/p is replaced by normalized equivalent shear stress, $q = \sqrt{3(S_{ij}/p' - S_{ij_0}/p'_0)(S_{ij}/p' - S_{ij_0}/p'_0)/2}$, where S_{ij} = deviatoric stress tensor and the subscript "o" = variables relate to past consolidation history. The function allows the yield surface to be inclined at the origin of the stress space at the start of shearing. It does not rotate further with shearing, Prevost (1978) and Mroz et al. (1978) also presented an anisotropic model that accounted for induced anisotropy, but it was based on the nested surface associated with a kinematic hardening rule.

Anandarajah and Dafalias (1985, 1986) and Liang and Ma (1992) introduced induced stress invariants based on the fabric tensor to replace the corresponding stress invariants in the yield function of the modified Cam-clay model. The models were based on bounding surface plasticity. The isotropic, anisotropic and distortional hardening rules were used to describe the evolution of the bounding surface as plastic strain develops. The projection center of the bounding surface is set along the induced hydrostatic line.

Dafalias (1987) proposed an anisotropic theory based strictly on the critical state concept. An anisotropic dissipating energy measurement α was introduced in the triaxial space. The theory was generalized into three-dimensional stress space by assuming $\alpha = \sqrt{2}\alpha_{ij}\alpha_{ij}/3$, which expresses the yield function in terms of anisotropic tensor (see the equation in Table 1). When $\alpha = 0$, the function reduces to that of the modified Cam-clay model. Crouch and Wolf (1992) further introduced a constant shape parameter to the yield function in order to control the tensile strength. Crouch and Wolf (1995) generalized the model into three-dimensional stress space but no validation was presented. Both models of Crouch assumed a constant shape parameter and did not consider distortional hardening. The models were also expressed with the bounding surface theory having the projection center at the origin of the stress space (Crouch et al. 1994).

The MIT series of soil models (Whittle 1993; Whittle and Kavvas 1994) are extensions of the modified Cam-clay model. The equivalent shear stress is defined as $q = \sqrt{3}(S_{ij} - p\alpha_{ij})(S_{ij} - p\alpha_{ij})/2$, where α_{ij} = anisotropic tensor that changes with the plastic strain. Thus, unlike Ohta's model, MIT models allow rotation of yield surface during subsequent shearing. In order to capture the critical state, a nonassociated flow rule

was adopted. Thus the key features of the MIT-E1 model include an anisotropic yield surface, kinematic plasticity, and the capturing of strain-softening behavior under undrained conditions. Two additional features were incorporated in the MIT-E3 model: small strain nonlinear elasticity using a closed loop hysteric stress-strain formulation, and the bounding surface plasticity to model an overconsolidated clay behavior.

Banerjee and Yousif (1986) proposed an anisotropic model with the yield surface aligned along the K_0 line. The yield function was developed from the experimental results. The isotropic and anisotropic hardening rules were used. The isotropic hardening rule used in the model was the same as that of the modified Cam-clay model, whereas the anisotropic/rotational hardening rule was expressed as an empirical function that captures the critical state of soils.

This paper presents a generalized constitutive model for anisotropic cohesive soils using the concept of bounding surface plasticity and the critical state concept. The main features of the proposed model include a function for the bounding surface, hardening rules, plastic modulus, mapping rule, and constitutive equations. The model is verified with the test results of Kaolin Clay, San Francisco Bay Mud, and Boston Blue Clay. The time-dependent behavior is not included in the formulation presented herein.

Formulations

The model is a modification of the Kaliakin–Dafalias model (Kaliakin 1985; Kaliakin and Dafalias 1990) but the bounding surface is based on the extended anisotropic critical state theory (Dafalias 1987). Meanwhile, the rate effect is not included in this paper. Associated flow rule is used in the proposed model so that it is computationally less sophisticated than the kinematic models, while the most important features of anisotropic soil behavior can still be captured. Note that the plasticity model with nonassociated flow rule does not satisfy Drucker's postulate, thus the resulting solution may not be unique. Note that the anisotropy involved in the formulation focused on the initial and induced stress anisotropy. Structural anisotropy due to soil fabric structure is not part of the proposed formulation.

Bounding Surface

In the bounding surface theory, F is defined as a function of the stress tensor σ_{ij} and plastic internal variables q_n . That is, $F(\bar{\sigma}_{ij}, q_n) = 0$. The bar over the stress quantity denotes an image point on the bounding surface. The real stress point σ_{ij} within the bounding surface is related to the image stress point $\bar{\sigma}_{ij}$ on the bounding surface through a mapping rule. The direction of plastic loading–unloading is defined as the gradient of F at $\bar{\sigma}_{ij}$. A relation between the plastic modulus K_p and a bounding plastic modulus \bar{K}_p is established as a function of the Euclidean distance δ between σ_{ij} and $\bar{\sigma}_{ij}$.

In this study, the bounding surface is obtained by extending the critical state concept of Dafalias (1987) into three-dimensional stress states, and dependent on the reduced Lode angle through a function χ . That is,

$$F(\bar{\sigma}_{ij}, \alpha_{ij}, I_0, R) = (\bar{I} - I_0) \left(\bar{I} + \frac{R-2}{R} I_0 \right) + (R-1)^2 \frac{\bar{J}_a^2}{\chi/27} = 0 \quad (1a)$$

$$\bar{I} = \bar{\sigma}_{ij} \delta_{ij} \quad (1b)$$

$$\bar{S}_{ij} = \bar{\sigma}_{ij} - \bar{\sigma}_{kk} \delta_{ij}/3 \quad (1c)$$

$$\bar{S}_{ij}^a = \bar{S}_{ij} - \bar{\sigma}_{kk} \alpha_{ij}/3 \quad (1d)$$

$$\bar{J}_a^2 = \bar{S}_{ij}^a \bar{S}_{ij}^a / 2 \quad (1e)$$

$$\bar{S}_a^3 = \bar{S}_{ij}^a \bar{S}_{jk}^a \bar{S}_{ki}^a / 3 \quad (1f)$$

$$\sin 3\bar{\theta} = \frac{3\sqrt{3}}{2} \left(\frac{\bar{S}_a}{\bar{J}_a} \right)^3 \quad \left(-\frac{\pi}{6} \leq \bar{\theta} \leq \frac{\pi}{6} \right) \quad (1g)$$

$$\chi(\bar{\theta}) = \frac{2k}{1+k-(1-k)\sin 3\bar{\theta}} \chi_c \quad (1h)$$

$$k = \chi_e / \chi_c \quad (1i)$$

$$\chi_c = f(M_c, \alpha, R) \quad (1j)$$

$$\chi_e = f(M_e, \alpha, R) \quad (1k)$$

$$f(M, \alpha, R) = \frac{M-\alpha}{2} [2\alpha(R-1)^2 + M - \alpha + \sqrt{4\alpha(R-1)^2 M + (M-\alpha)^2}] \quad (1l)$$

$$\alpha = \sqrt{\frac{3\alpha_{ij}\alpha_{ij}}{2}} \quad (1m)$$

where \bar{I} , \bar{S}_{ij} , \bar{S}_{ij}^a , \bar{J}_a , \bar{S}_a , and $\bar{\theta}$ = first stress invariant, deviatoric stress tensor, reduced deviator stress tensor, reduced second stress invariant, reduced third stress invariant, and reduced Lode angle, respectively. A superposed bar indicates that the variables are related to the bounding surface. Parameters α , α_{ij} , M , and R = anisotropic measurement, anisotropic tensor, slope of critical state line in triaxial space, and shape parameter, respectively, and δ_{ij} = Kronecker data.

The anisotropic tensors α_{ij} are expressed through a constant A_0 with the initial stress states

$$\alpha_{ij}^0 = A_0 \frac{S_{ij}^0}{p_0} \quad (2a)$$

$$S_{ij}^0 = \sigma_{ij}^0 - p_0 \delta_{ij} \quad (2b)$$

With the initial stress ratio $K_0 = \sigma_{30}/\sigma_{10}$, the anisotropic tensors are given as follows:

$$\alpha_{11}^0 = 2k^0, \quad \alpha_{22}^0 = \alpha_{33}^0 = -k^0, \quad \alpha_{12}^0 = \alpha_{23}^0 = \alpha_{13}^0 = 0 \quad (2c)$$

$$k^0 = A_0 \frac{1-K_0}{1+2K_0} \quad (2d)$$

For isotropically consolidated specimens $K_0 = 1.0$, thus $k^0 = 0$. For the K_0 -consolidated specimen, $A_0 = 0.65-1.0$ (e.g., Liang and Ma 1992).

R controls the shape of the bounding surface. In this proposed model, R is considered to vary with volumetric strain. A flatter shape is obtained by increasing the value of R . When R is equal to 2, the surface degenerates to that proposed by Dafalias (1987). The surface also exhibits a unique property not available in existing anisotropic models such that at the end of anisotropic consolidation, the stress state is at the right tip of the yield surface [Fig. 1(a)]. That is $I_0/3$ is the largest mean effective stress the soil element has experienced after K_0 consolidation, whether it is in the state of neutral loading or unloading.

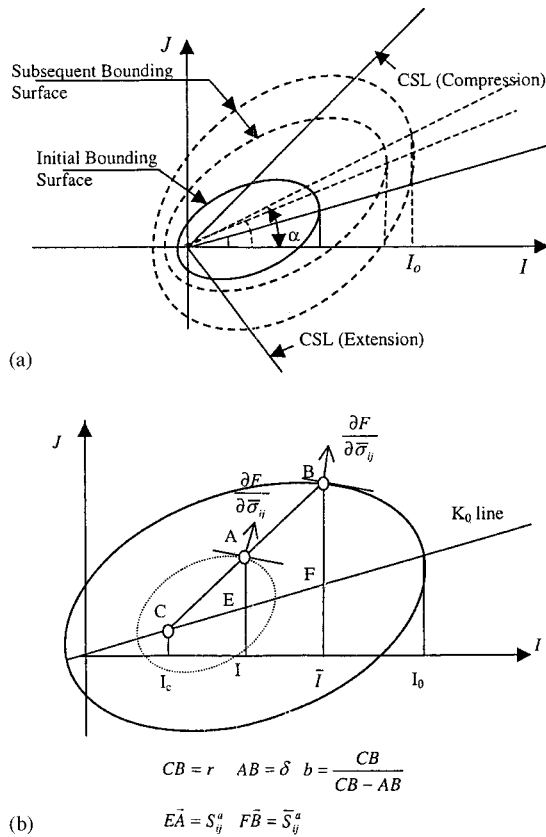


Fig. 1. Anisotropic model: (a) bounding surface and (b) mapping rule

The normal to the bounding surface at its intersection with the critical state line is parallel to the \bar{J} axis. Thus the bounding surface allows an associated flow rule to be used for determining the direction of plastic strain rate, while also predicting the critical state for strain hardening soils. The approach is less sophisticated than MIT models, for example, which adopt a nonassociated flow rule combined with an additional failure curve for predicting the failure state.

Hardening Rules

The isotropic, rotational/anisotropic, and distortional hardening rules are used to control the size, rotation, and distortion of the bounding surface. The hardening equations are expressed for the associated flow rule.

Isotropic Hardening Rule

The bounding surface expands, contracts, or remains unchanged in size depending on the plastic volumetric strain rate. The evolution of I_0 is determined from the following equations:

$$\dot{I}_0 = \frac{1+e_0}{\lambda-\kappa} (\langle I_0 - I_L \rangle + I_L) \langle L \rangle R_{kk} \quad (3a)$$

$$R_{kk} = \delta_{ij} R_{ij} \quad (3b)$$

$$R_{ij} = \frac{\partial F}{\partial \sigma_{ij}} \quad (3c)$$

where λ and κ are obtained from the slope of the primary compression and swelling lines in the $e - \ln p$ relationships of isotropic consolidation; L = loading function that governs the magni-

tude of plastic strain [see Eqs. (6a) and (6b)]; $\langle \rangle$ = Macaulay brackets which implies that $\langle L \rangle = L$ if $L > 0$ and $\langle L \rangle = 0$ if $L \leq 0$; F = analytical expression for the bounding surface; and R_{ij} = gradient of plastic potential. e_0 and I_0 (where $I_0 = 3p_0$) = initial void ratio and preconsolidated stress conditions. I_L is used for computational stability at low value of I so that e versus p relationship changes from logarithmic to linear (Dafalias and Hermann 1986). Its value is typically assigned as one-third atmospheric pressure.

Rotational/Anisotropic Hardening Rule

The rotational rate of the bounding surface is controlled by the evolution of the anisotropic tensor. Experimental results (e.g., Morgenstern and Tchalenko 1967; Mitchell 1970) revealed that the rate of anisotropy is influenced by the stress increments but not by the absolute value of the stress. If an anisotropic specimen is sheared continuously, the initial anisotropy may be erased. Also, a saturation state is obtained at the critical state so that isotropic and anisotropic specimens exhibit the same behavior. The following expression is used to accommodate for such anisotropic behavior:

$$\dot{\alpha}_{ij} = \Lambda_1 \frac{1+e_0}{\lambda-\kappa} \bar{S}_{ij}^a \langle L \rangle R_{kk} \quad (4a)$$

where

$$\Lambda_1 = \frac{\psi_1 \xi}{I_0} \exp\left(-\psi_2 \frac{\rho}{|\rho|} (1+\rho)\alpha\right) \quad (4b)$$

$$\xi = \left\langle 1.0 - \frac{\bar{J}}{N|\bar{I}|} \right\rangle \quad (4c)$$

$$\rho = \frac{\alpha_{ij}}{\sqrt{\frac{2}{3}}\alpha} R_{ij}^S \quad (4d)$$

$$R_{ij}^S = \frac{R_{ij} - \frac{1}{3} R_{mn} \delta_{mn} \delta_{ij}}{|R_{ij}|} \quad (4e)$$

where ψ_1 and ψ_2 = positive constants. Parameter N = slope of the critical state line in I - J stress space and I_0 is introduced to normalize Eq. (4b). Parameter ξ is used to capture the anisotropic saturation for generalized stress conditions and a heavily consolidated specimen and ρ accounts for the change in the loading direction with respect to the anisotropic tensor (Anandarajah and Dafalias 1985, 1986). For proportional loading paths, $\bar{S}_{ij}^a = 0$, so the rate of anisotropy ($\dot{\alpha}_{ij}$) is equal to zero. Also, at critical state, $\bar{J}/|\bar{I}| = N$, thus $\dot{\alpha}_{ij} = 0$.

Distortional Hardening Rule

R is a parameter used to control the ratio of J versus I in the bounding surface. The following equation is adopted from Anandarajah and Dafalias (1985, 1986) in accounting for distortional hardening:

$$\dot{R} = \Lambda_2 \frac{1+e_0}{\lambda-\kappa} \langle L \rangle R_{kk} \quad (5a)$$

$$\Lambda_2 = -\psi_1 \psi_3 \xi \left(\frac{J_a}{I_0} \right)^2 \exp\left(-\psi_2 \frac{\rho}{|\rho|} (1+\rho)\alpha\right) \quad (5b)$$

Bounding Plastic Modulus

The proposed model obeys the associated flow rule. Therefore the yield function also serves as the plastic potential function. The plastic strain rate is determined as

$$\dot{\varepsilon}_{ij}^p = \langle L \rangle \frac{\partial F}{\partial \bar{\sigma}_{ij}} \quad (6a)$$

$$L = \frac{1}{\bar{K}_p} \frac{\partial F}{\partial \bar{\sigma}_{ij}} \dot{\sigma}_{ij} = \frac{1}{K_p} \frac{\partial F}{\partial \sigma_{ij}} \dot{\sigma}_{ij} \quad (6b)$$

where L , K_p , and \bar{K}_p = plastic loading index, and the plastic moduli at current stress state and image stress states, respectively.

Substituting the hardening rules and loading index into the consistency conditions, the bounding plastic modulus is obtained as

$$\begin{aligned} \bar{K}_p = & -\frac{1+e_0}{\lambda-\kappa} \left[\langle (I_0 - I_L) + I_L \rangle \frac{\partial F}{\partial I_0} + \Lambda_1 \frac{\partial F}{\partial \alpha_{ij}} \bar{S}_{ij}^a \right. \\ & \left. + \Lambda_2 \frac{\partial F}{\partial R} \right] R_{kk} \quad (7a) \end{aligned}$$

The plastic modulus is related to the bounding plastic modulus through the following relationships:

$$K_p = \bar{K}_p + \frac{1+e_0}{\lambda-\kappa} p_a R_{ij} R_{ij} \left(\frac{\delta}{\langle r-sb \rangle} \right)^W \quad (7b)$$

where the variables b , s , r , and δ are illustrated in Fig. 1(b). They are used to relate the actual and image stress points, and to define the extent of elastic nucleus, radial distance, and Euclidean distance in the stress space, respectively. p_a = atmospheric pressure. W = positive constant which is introduced to replace the parameters h_e , h_c , and z used in the plastic modulus of earlier versions of the bounding surface model. The comparison as presented subsequently showed that the accuracy of predictions is not sacrificed significantly by reducing the number of parameters in the expression.

Mapping Rule

In the proposed model, the projection center is formulated to move along the K_0 line rather than at the origin of I - J stress space. The image stress variables are related through the actual stress variables using the radial mapping rule [Fig. 1(b)]. That is

$$\sigma_{ij}^C = \frac{1}{3} C I_0 (\alpha_{ij} + \delta_{ij}) \quad (8a)$$

where C ($0 \leq C \leq 1$) = material constant. C defines the point along the K_0 line which serves as the projection center in the radial mapping rule, thus it determines the mapped actual stress of the bounding surface. It affects the dilation and contraction of soils, but does not affect the material response for states lying on the bounding surface. The elastic nucleus has the projection center as its center of homology, thus C affects the magnitude of K_p .

From geometry, the following relationships are used in relating current stress states to those at the bounding surface:

$$\begin{aligned} \bar{I} &= b(I - CI_0) + CI_0; \quad \bar{S}_{ij}^a = bS_{ij}^a; \quad \bar{J}_a = bJ_a; \\ \bar{S}_a &= bS_a; \quad \bar{\theta} = \theta \quad (8b) \end{aligned}$$

$$b = \frac{r}{r-\delta} \quad (8c)$$

where b , r , and δ are defined earlier [Fig. 1(b)].

The projection center is also an internal variable. By substituting the isotropic and anisotropic hardening rules into the derivative of above equation, the evolution of the projection center becomes

$$\dot{\sigma}_{ij}^C = \frac{1}{3} C \frac{1+e_0}{\lambda-\kappa} [\langle (I_0 - I_L) + I_L \rangle (\alpha_{ij} + \delta_{ij}) + \Lambda_1 \bar{S}_{ij}^a] \langle L \rangle R_{kk} \quad (8d)$$

The change of the bounding surface with the internal variables is shown in Fig. 1(a).

Constitutive Equation

The total strain rate is assumed to be composed of two parts: elastic and plastic. That is

$$\dot{\varepsilon}_{ij} = \dot{\varepsilon}_{ij}^e + \dot{\varepsilon}_{ij}^p = C_{ijkl} \dot{\sigma}_{kl} + \langle L \rangle \frac{\partial F}{\partial \bar{\sigma}_{ij}} \quad (9)$$

where C_{ijkl} = fourth order tensor of elastic compliance. The associated flow rule is assumed which with the above presented expressions gives

$$\begin{aligned} \frac{\partial F}{\partial \bar{\sigma}_{ij}} = & \frac{\partial F}{\partial I} \delta_{ij} + \frac{1}{2J_a} \frac{\partial F}{\partial \bar{J}_a} \left(S_{ij}^a - \frac{1}{3} \delta_{ij} \alpha_{ij} S_{ij}^a \right) \\ & + \frac{\sqrt{3}}{2\bar{J}_a \cos 3\theta} \frac{\partial F}{\partial \theta} \left[\frac{1}{\bar{J}_a} \left(S_{ik} S_{kj} - \frac{3}{2} \frac{S_a^3}{J_a^2} S_{ij}^a \right) \right. \\ & \left. - \frac{2}{3} \delta_{ij} + \frac{\alpha_{ij} \delta_{ij}}{3J_a^2} \left(\frac{3}{2} \frac{S_a^3}{J_a^2} S_{ij}^a - S_{jk} S_{ki} \right) \right] \quad (10) \end{aligned}$$

The normal to the bounding surface is decomposed into hydrostatic and deviatoric components. The elastoplastic constitutive equation is thus expressed as

$$\begin{aligned} \dot{\sigma}_{ij} = & 2G \dot{\varepsilon}_{ij} + (K - \frac{2}{3}G) \dot{\varepsilon}_{kk} \delta_{ij} - \langle L \rangle \\ & \times [2GR_{ij} + (K - \frac{2}{3}G) R_{kk} \delta_{ij}] \quad (11) \end{aligned}$$

where K and G = bulk and shear moduli, respectively. Note that K is related to κ as $K = (1+e)p/\kappa$. The constitutive model was implemented into CALBR8 (Kaliakin 1992) for simulating the response using a single element. Note that the simulation presented here adopted a reformulated analysis (Herrmann 1965) for undrained conditions using the bulk modulus of water, where the stiffness of the composite material is due to a combination of material skeleton and pore water. Since water does not transmit shear, the stiffness of water is entirely due to its bulk modulus of compressibility.

Parameters

The proposed model requires 12 material parameters as well as the initial stress state parameters (e_0 , A_0 , p_0 , and initial given components). The parameters are related to critical state soil mechanics (λ , κ , M_c , M_e , G , or ν), bounding surface configurations (R , C , s), and hardening functions (ψ_1 , ψ_2 , ψ_3 , W).

λ and κ are obtained from isotropic consolidation tests. They may also be obtained from the compression and swelling indexes (C_c and C_s) of one-dimensional consolidation tests where $\lambda = 0.434C_c$ and $\kappa = 0.434C_s$. M , which may be different for compression and extension tests (denoted as M_c and M_e), is obtained

Table 2. Material Parameters for Kaolin Clay, San Francisco Bay Mud, and Boston Blue Clay

| Parameters | Kaolin Clay | San Francisco Bay Mud | Boston Blue Clay |
|------------------------------|---------------------------------------|--------------------------------------|---------------------------------------|
| Traditional | | | |
| λ | 0.14 ^a | 0.37 ^b | 0.175 ^c |
| κ | 0.05 ^a | 0.054 ^b | 0.034 ^c |
| ν | 0.20 ^a | 0.2 ^b | 0.227 ^c |
| M_c, M_e | 1.05 ^a , 0.78 ^a | 1.4 ^b , 1.12 ^b | 1.39 ^c , 1.12 ^c |
| Surface configuration | | | |
| R | 2.6 | 2.8 | 3.6 |
| C | 0.23 | 0.23 | 0.23 |
| S | 1.5 | 1.5 | 1.5 |
| Hardening | | | |
| ψ_1 | 20 | 100 | 20 |
| ψ_2 | 10 | 10 | 10 |
| ψ_3 | 80 | 50 | 100 |
| W | 2.0 | 2.0 | 2.0 |

^aBanerjee and Yousif (1986); Stipho (1978).

^bBonaparte (1981).

^cWhittle (1993).

from the slope of the critical state line or indirectly from the angle of internal friction ϕ . G may be specified as a constant (obtained from K and ν) or a variable dependent on the stress levels.

Undrained stress path of the normally consolidated soil may be used to obtain the initial value of R , where 2.0 is a typical value. C is obtained from the test results of lightly to highly overconsolidated specimens under undrained shearing. s ($1 \leq s \leq \infty$) = elastic zone parameter, with $s = 1$ leading to inelastic behavior at any point within the bounding surface and $s = \infty$ or any large value showing a purely elastic behavior within the surface so that the bounding surface behaves like a classical yield surface.

ψ_1 , ψ_2 , and ψ_3 are obtained by best fitting the experimental results, typically for the normally consolidated isotropic compression and extension tests, and then extended to the normal and overconsolidated anisotropic tests.

The calibration is described subsequently for several types of clay and compared with reported experimental results.

Validations

The model was calibrated and verified with three different types of clay: Kaolin Clay (Stipho 1978), Boston Blue Clay (Ladd and

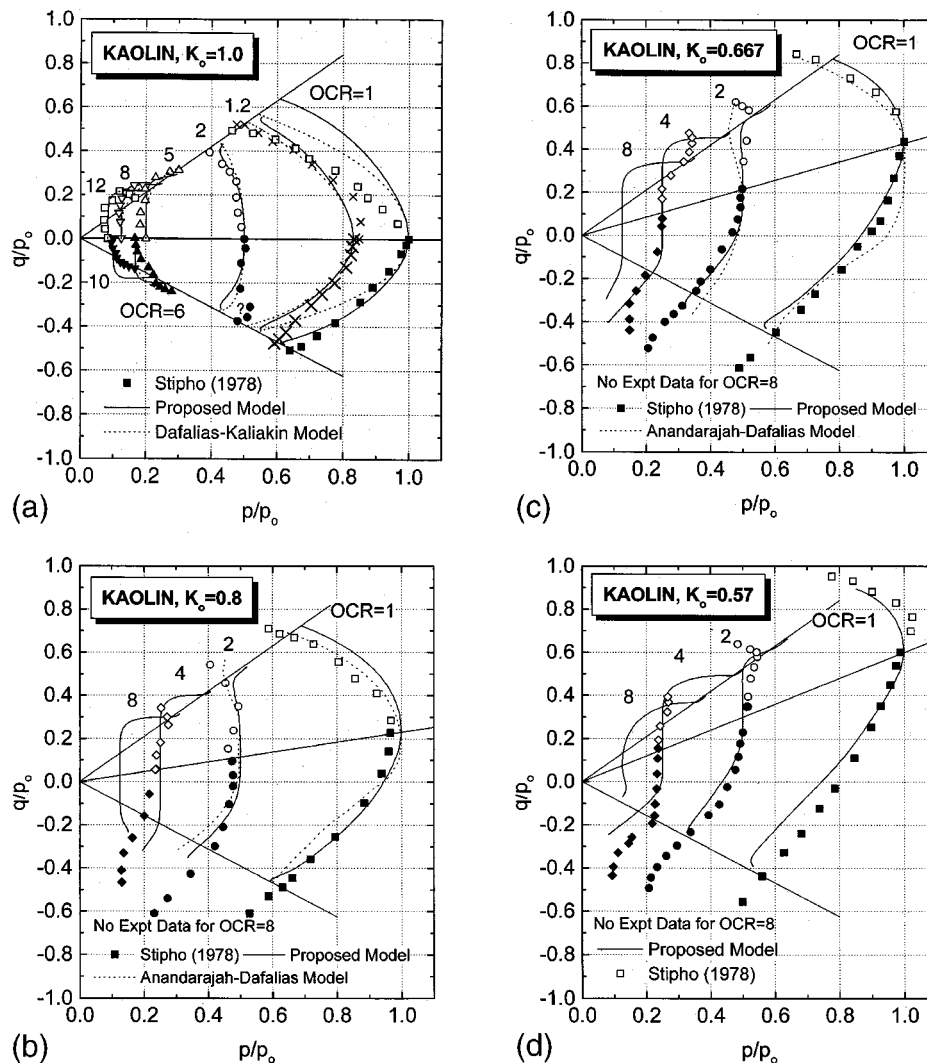


Fig. 2. Comparison of stress paths for Kaolin Clay: (a) $K_0=1.0$, (b) $K_0=0.8$, (c) $K_0=0.67$, and (d) $K_0=0.57$

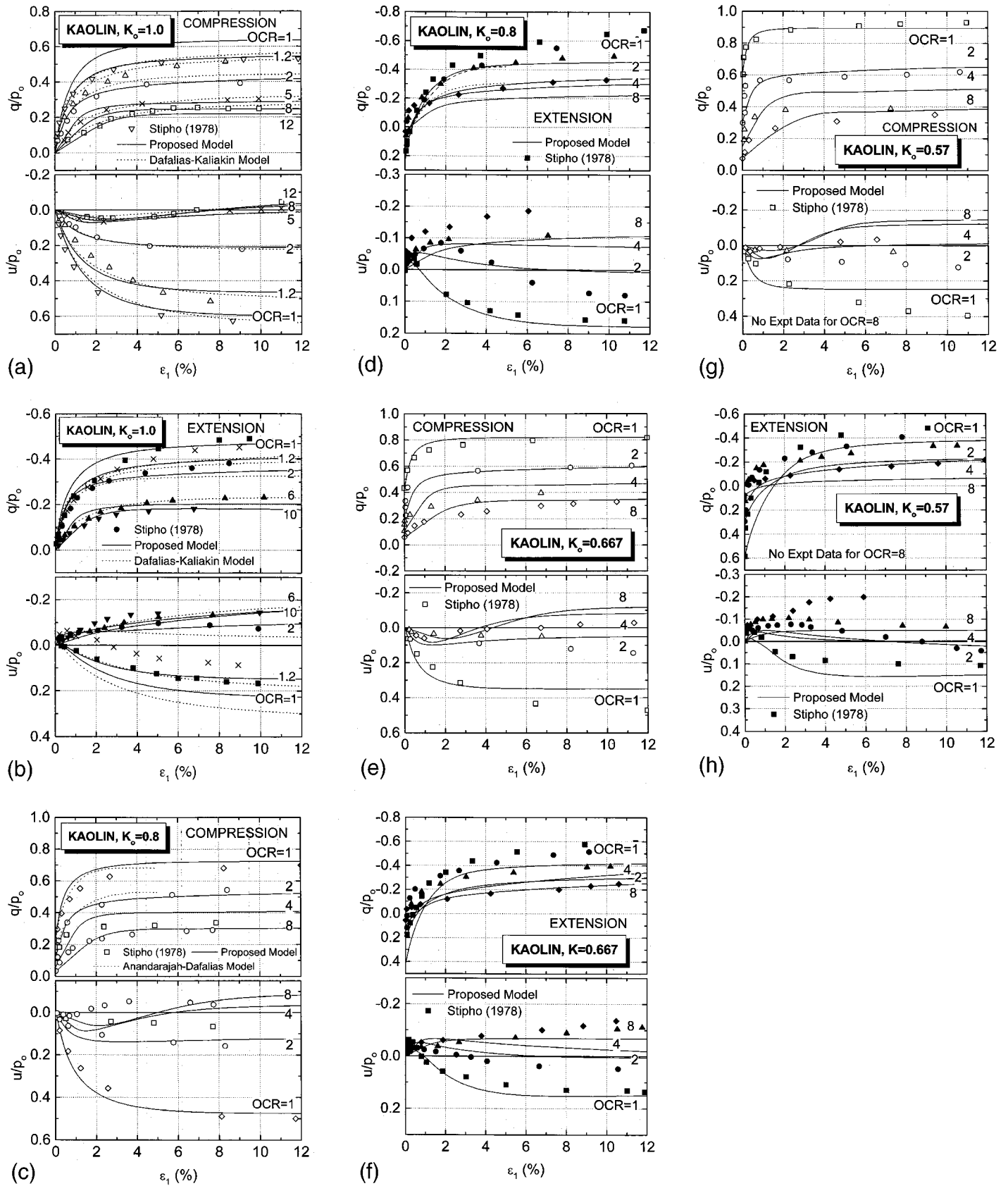


Fig. 3. Comparison of stress-strain and excess pore water pressure response for Kaolin Clay: (a) compression $K_0=1.0$, (b) extension $K_0=1.0$, (c) compression $K_0=0.8$, (d) compression $K_0=0.667$, and (e) extension $K_0=0.57$

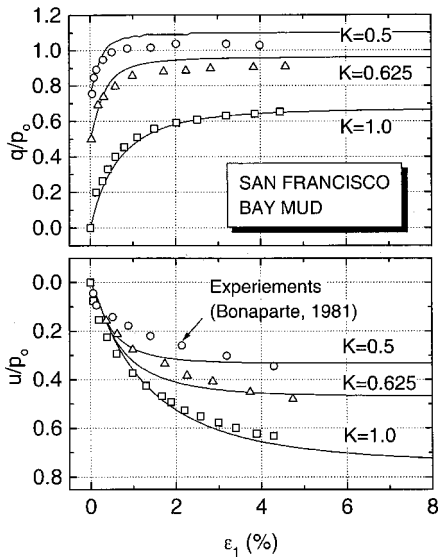


Fig. 4. Comparison for San Francisco Bay Mud: Stress–strain and excess pore water pressure response

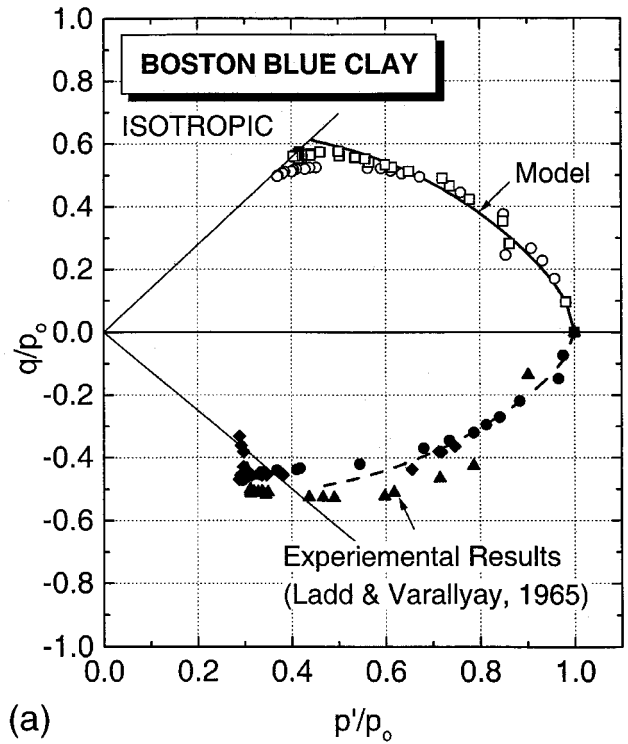
Vallayay 1965), and San Francisco Bay Mud (Bonaparte 1981). The calibration of material parameters was based on the results of isotropically consolidated specimens, so that the behavior of anisotropically consolidated specimens were predicted. Table 2 summarizes the parameters and their values.

Kaolin Clay

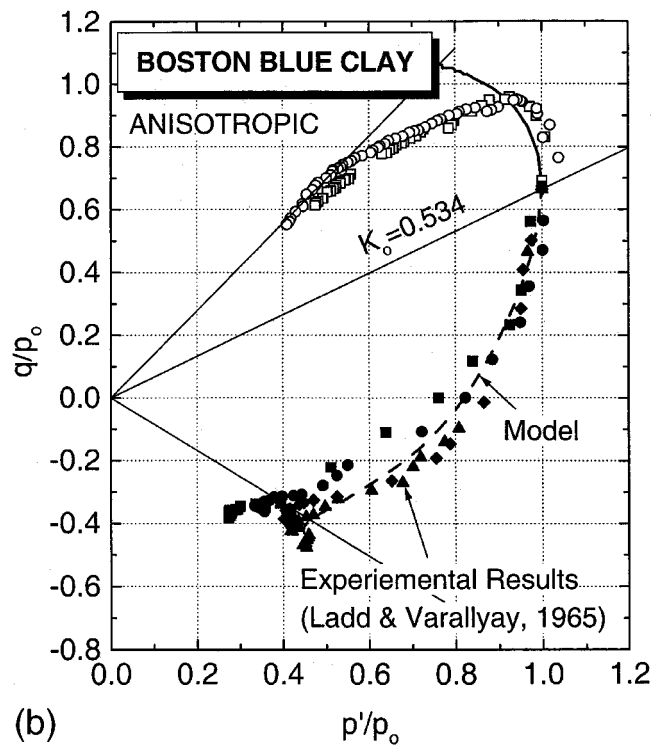
The series of undrained shearing tests were conducted on isotropically and anisotropically consolidated specimens (Stipho 1978) with the overconsolidation ratio (OCR) ranging from 1.0 to 8.0 for isotropic tests and 1.0–4.0 for anisotropic tests ($K_0=1.0, 0.8, 0.67,$ and 0.57) under triaxial compression and extension conditions. The value of initial void ratio e_0 was between 0.94 to 1.07 while the preconsolidation stress p'_0 was between 357 and 408 kPa for isotropically consolidated tests and 204 kPa for anisotropically consolidated tests. Note that these tests were stress controlled and the failure state may not be properly captured. Several researchers have used the results for verifying their constitutive models (e.g., Anandarajah and Dafalias 1986; Banerjee and Yousif 1986; Liang and Ma 1992). In the validation here, the values of traditional critical state parameters were based on the isotropic test results (Stipho 1978). The surface configuration parameters (R and S) were obtained by best fitting the stress paths and stress–strain response of isotropic, lightly overconsolidated specimens with $OCR=1.2$. C was calibrated from the isotropic, highly overconsolidated specimens at $OCR=5.0$. The hardening parameters (ψ_1, ψ_2, ψ_3) were calibrated from normally consolidated specimens at $K_0=0.8$ for both compression and extension conditions.

Figs. 2(a–d) show the comparisons for the stress paths obtained from the tests and model simulations. The comparisons for corresponding deviatoric stress and excess pore pressure versus strain response are shown in Figs. 3(a–h). The results determined from Kaliakin–Dafalias’ model at $K_0=1.0$ and Anandarajah–Dafalias’ model at $K_0=0.8$ and 0.667 are also shown. The model was able to predict the response over a wide range of K_0 (from 0.57 to 1.0) and OCR (from 1.0 to 8.0).

There were some notable differences between the behavior of isotropically and anisotropically consolidated tests as observed



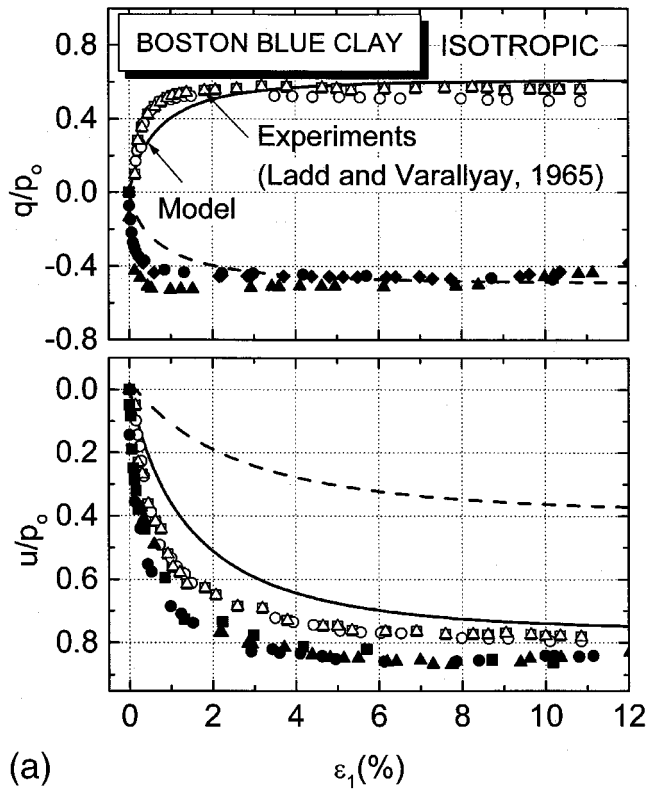
(a)



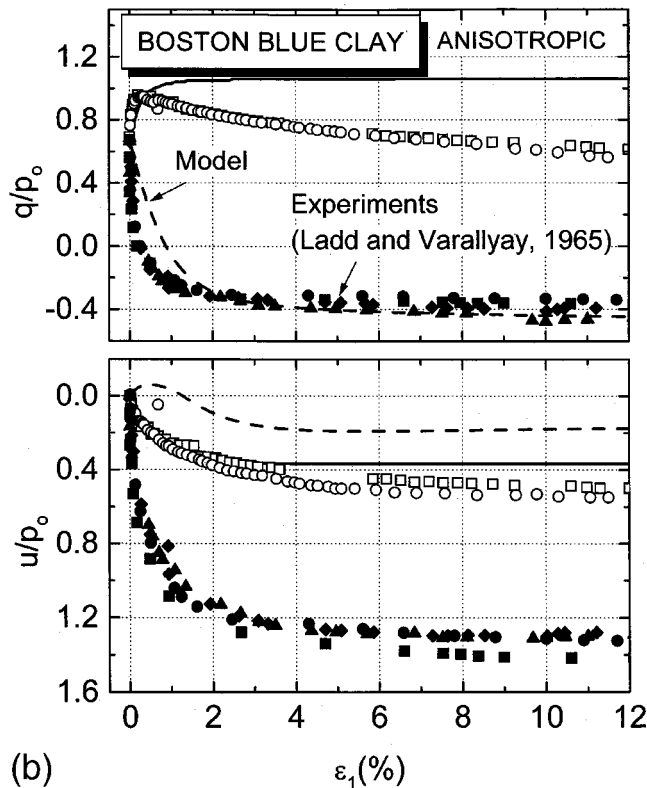
(b)

Fig. 5. Comparison of stress paths for Boston Blue Clay: (a) $K_0=1.0$ and (b) $K_0=0.534$

experimentally and also predicted by the model. For specimens consolidated isotropically with moderate overconsolidation ratio, such as $OCR=2$ or less, the stress path shows a reduction in p until it reached the critical state line. For isotropically consolidated specimens with high overconsolidation ratio, such as $OCR=5$ or above, the stress path gave an abrupt increase in q with little change in p until it passed beyond the critical state line,



(a)



(b)

Fig. 6. Comparison of stress–strain and excess pore water pressure response for Boston Blue Clay: (a) $K_0=1.0$ and (b) $K_0=0.534$

and then an increase in p until it touched the critical state line. Such behavior of highly overconsolidated specimens was observed at much lower overconsolidation in anisotropically consolidated specimens, such as that with $OCR=2$. The negative ex-

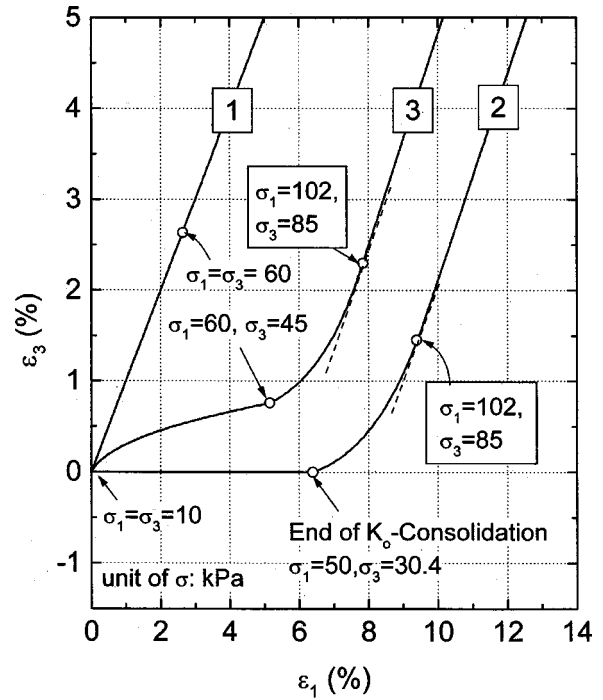


Fig. 7. Erase of anisotropy-memory during isotropic consolidation tests

cess pore pressure at high OCR and under extension mode was also predicted by the proposed model. The strength anisotropy in compression and extension modes was also captured.

The results of predictions indicated that the model using a simplified form of plastic modulus did not result in significantly different results for normally consolidated soils. The model gave a better prediction for overconsolidated clays, especially at higher OCR and extension mode compared to Kaliakin–Dafalias’ model. It also gave more satisfactory prediction for the anisotropic tests,

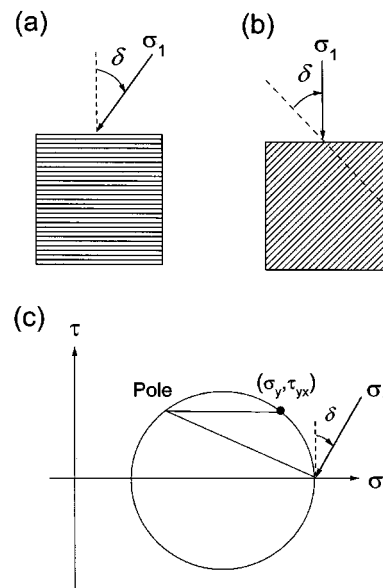


Fig. 8. Inherent anisotropy denoted by inclination of major principal stress

at high OCR, for the extension test compared to the results obtained by Anandarajah and Dafalias (1986) and Liang and Ma (1992).

San Francisco Bay Mud

Bonaparte (1981) conducted a series of undrained tests on isotropically and anisotropically consolidated specimens of San Francisco Bay Mud. The initial void ratio was $e_0 = 1.35$ for all specimens. In these tests, $p_0 = 100, 353.16, \text{ and } 130.8 \text{ kPa}$ for $K_0 = 1.0, 0.65, \text{ and } 0.5$, respectively. The results were limited to normally consolidated specimens and for compression mode, thus some parameters related to OCR, such as W and C , were assigned values similar to Kaolin Clay. In fact these two parameters did not affect the response significantly. The values of traditional parameters were given by Bonaparte (1981). The series of isotropic test results have been used extensively to verify constitutive models (e.g., Borja and Kavazanjian 1985). Fig. 4 shows the comparison between the experimental and simulated results for the deviatoric stress–axial strain and excess pore pressure–axial strain relationships. The simulations are considered satisfactory.

Boston Blue Clay

Ladd and Varallyay (1965) performed a series of undrained triaxial compression and extension tests on isotropically and anisotropically ($K_0 = 0.534$) normally consolidated Boston Blue Clay. The specimens were tested at $e_0 = 0.84\text{--}0.89$ and p_0 ranging from 273 to 785 kPa. The traditional parameters are given by Whittle (1993). Since no overconsolidated isotropic specimens were tested, the parameters W and C were assigned with values similar to Kaolin Clay and San Francisco Bay Mud. Figs. 5 and 6 compare the results of simulations with the experimental results. The solid and dashed lines show the predicted results for compression and extension tests, respectively. The closed and open points are the experimental results for compression and extension tests, respectively. The predicted stress paths are satisfactory for the isotropic tests and anisotropic extension tests. The prediction for anisotropic compression tests was less satisfactory because of strain softening behavior, which may be overcome with a kinematic hardening approach like the MIT models. However, the excess pore pressure was underestimated in the extension tests, though the experimental value seems extremely large.

Other Aspects of Anisotropy

Erase of Anisotropy Memory

Anandarajah and Dafalias (1985, 1986) investigated the behavior of their bounding surface model for initially anisotropic specimens when subject to isotropic consolidation. For isotropically consolidated specimens, the major and minor principal strains are the same, i.e., $\varepsilon_1 = \varepsilon_3$. However, for initially anisotropic specimens, the major and minor principal strains are not the same until the stress level has been increased to 1.5–2.5 times the initial stress. The fabric still remains anisotropic although the response is isotropic (Anandarajah et al. 1996). That is, the memory of anisotropy was erased by subsequent isotropic consolidation. Fig. 7 shows three case studies using the properties of Kaolin Clay. Case 1 considered an isotropic consolidation. For Case 2, the specimen was consolidated anisotropically to a stress state of $\sigma_3 = 35 \text{ kPa}$ and $\sigma_1 = 50 \text{ kPa}$ followed by isotropic consolidation. K_0 consolidation was conducted in Case 3 until $\sigma_1 = 50 \text{ kPa}$, where

σ_3 was obtained as 30.4 kPa. The specimen was then consolidated isotropically. The results showed that during the initial portion of subsequent isotropic consolidation of specimens in Cases 2 and 3, $\Delta\varepsilon_3$ was smaller than $\Delta\varepsilon_1$. However, as the stress level exceeded 1.8, $\Delta\varepsilon_1 = \Delta\varepsilon_3$ and the behavior resembled that of an initially isotropic specimen. Thus, the proposed model is capable of simulating erase of memory for an anisotropically consolidated specimen when subject to isotropic consolidation.

Inherent Anisotropy

The simulation capability of the proposed model has been focused mainly on stress anisotropy. It has to be noted that the model is capable of modeling the inherent anisotropy of clay due to the different orientation of the direction of major principal stress with the axis of deposition, δ [Fig. 8(a)]. In fact, the compression and extension tests are two typical cases with $\delta = 0$ and 90° , respectively. However, testing with other angles of inclination requires a special device such as a directional shear apparatus by applying appropriate shear stress after achieving anisotropic stress states [Fig. 8(c)]. δ may be controlled to be constant or to rotate during subsequent shearing. The tests with specially prepared specimens having an inclined plane of deposition [Fig. 8(b)] do not allow rotation of major principal stress.

Summary and Conclusions

A constitutive model, based on the critical state concept and bounding surface plasticity, has been developed to simulate stress anisotropy in clay. A simplified form of the plastic modulus was used. The model considered isotropic, rotational, and distortional hardenings using a total of 12 material parameters as well as the initial stress states. The comparisons with test results of three types of clay under different stress and overconsolidation ratios, and under compression and extension modes, revealed the predictive capability of the proposed model.

The model is limited to soils that do not exhibit significant strain-softening behavior. Test results with careful measurement of excess pore water pressure under extension mode are required for further validation. Since triaxial tests were used for calibration and validation, additional work should be conducted to verify the model with other modes of shearing, and also with the boundary-value problems.

References

- Anandarajah, A., and Dafalias, Y. F. (1985). "Anisotropic hardening bounding surface constitutive model for clays." *Proc., 5th Int. Conf. on Numerical Methods in Geomechanics*, Balkema, Rotterdam, The Netherlands, 267–275.
- Anandarajah, A. M., and Dafalias, Y. F. (1986). "Bounding surface plasticity. III: Application to anisotropic cohesive soils." *J. Eng. Mech.*, 112(12), 1292–1318.
- Anandarajah, A., Kuganenthira, N., and Zhao, D. (1996). "Variation of fabric anisotropy of kaolinite in triaxial loading." *J. Geotech. Eng.*, 122(8), 633–640.
- Banerjee, P. K., and Yousif, N. B. (1986). "A plasticity model for the mechanical behavior of anisotropically consolidated clay." *Int. J. Numer. Analyt. Meth. Geomech.*, 10, 521–541.
- Bonaparte, R. (1981). "A time-dependent constitutive model for cohesive soils." PhD thesis, Univ. of California, Berkeley, Calif.
- Borja, R. I., and Kavazanjian, E. (1985). "A constitutive model for the stress-strain-time behavior of wet clay." *Geotechnique*, 35(3), 283–298.

- Crouch, R. S., and Wolf, J. P. (1992). "A unified 3-dimensional anisotropic modular elliptic bounding surface model for soil." *Proc., 4th Int. Conf. on Numerical Models in Geomechanics*, Balkema, Rotterdam, The Netherlands, 137–147.
- Crouch, R. S., and Wolf, J. P. (1995). "On a three-dimensional anisotropic plasticity model for soil." *Geotechnique*, 45(2), 301–305.
- Crouch, R. S., Wolf, J. P., and Dafalias, Y. F. (1994). "Unifired critical state bounding surface plasticity model for soil." *J. Eng. Mech.*, 120(11), 2251–2270.
- Dafalias, Y. F. (1986). "Bounding surface plasticity. I: Mathematical foundation and hypoplasticity." *J. Eng. Mech.*, 112(9), 966–987.
- Dafalias, Y. F. (1987). "An anisotropic critical state clay plasticity model." *Constitutive laws for engineering materials: Theory and applications*, C. S. Desai et al., eds., 513–521.
- Dafalias, Y. F., and Herrmann, L. R. (1982). "Bounding surface formulation of soil plasticity." *Soil mechanics—Transient and cyclic loads*, G. N. Pande and D. C. Zienkiewicz, eds., Wiley, New York, 253–282.
- Dafalias, Y. F., and Herrmann, L. R. (1986). "Bounding surface plasticity. II: Application to isotropic cohesive soils." *J. Eng. Mech.*, 112(9), 1263–1291.
- DiMaggio, F. L., and Sandler, I. S. (1971). "Material model for granular soils." *J. Eng. Mech. Div.*, 97(3), 935–950.
- Drucker, D. C., Gibson, R. E., and Henkel, D. J. (1957). "Soil mechanics and work hardening theories of plasticity." *Trans. Am. Soc. Civ. Eng.*, 122, 338–346.
- Drucker, D. C., and Prager, W. (1952). "Soil mechanics and plastic analysis of limit design." *Q. Appl. Math.*, 10(2), 157–175.
- Duncan, J. M., and Seed, H. B. (1966). "Anisotropy and stress reorientation in clay." *J. Soil Mech. Found. Div., Am. Soc. Civ. Eng.*, 92(5), 21–50.
- Graham, J., Noonan, M. L., and Lew, K. V. (1983). "Yield states and stress-strain relationships in a natural plastic clay." *Can. Geotech. J.*, 20(3), 502–516.
- Herrmann, L. R. (1965). "Elastic equations for incompressible and nearly incompressible materials by a variational theorem." *Am. Inst. Aeronaut. Astronaut. J.*, 3(10), 1896–1900.
- Kaliakin, V. N. (1985). "Bounding surface elastoplasticity-viscoplasticity for clays." PhD thesis, Univ. of California, Davis, Calif.
- Kaliakin, V. N. (1992). *CALBR8*—A simple computer program for assessing the idiosyncrasies of various constitutive models used to characterize soils, Dept. of Civil Engineering, Univ. of Delaware, Newark, Del.
- Kaliakin, V. N., and Dafalias, Y. F. (1990). "Theoretical aspects of the elastoplastic-viscoplastic bounding surface model for isotropic cohesive soils." *Soils Found.*, 30(3), 11–24.
- Ladd, C. C., Foott, R., Ishihara, K., Schollosser, F., and Poulos, H. G. (1977). "Stress-deformation and strength characteristics." *Proc., 9th Int. Conf. on Soil Mechanics and Foundation Engineering*, Tokyo, 421–494.
- Ladd, C. C., and Varallyay, J. (1965). "The influence of the stress system on the behavior of saturated clays during undrained shear." *Research Rep. No. R65-11*, Dept. of Civil Engineering, MIT, Cambridge, Mass.
- Liang, R. Y., and Ma, F. (1992). "Anisotropic plasticity model for undrained cyclic behavior of clays. I: Theory." *J. Geotech. Eng.*, 118(2), 229–245.
- Lo, K. Y. (1965). "Stability of slopes in anisotropic soils." *J. Soil Mech. Found. Div., Am. Soc. Civ. Eng.*, 90(5), 133–155.
- Mitchell, R. J. (1970). "On the yielding and mechanical strength of Leda clay." *Can. Geotech. J.*, 7(3), 297–312.
- Morgenstern, N. R., and Tchaleako, J. S. (1967). "Microscopic structures in kaolin subjected to direct shear." *Geotechnique*, 27, 309–328.
- Mroz, Z., Norris, V. A., and Zienkiewicz, O. C. (1978). "An anisotropic hardening model for soils and its application to cyclic loading." *Int. J. Numer. Analyt. Meth. Geomech.*, 2, 203–221.
- Ohta, H., and Hata, S. (1971). "On the state surface of anisotropically consolidated clay." *Proc., Jpn. Soc. Civil Eng.*, 196, 117–124.
- Prevost, J. H. (1978). "Plasticity theory for soils stress-strain behavior." *J. Eng. Mech. Div.*, 104(5), 1177–1194.
- Roscoe, K. H., and Burland, J. B. (1968). "On the generalized strain-strain behavior of wet clay." *Engineering plasticity*, J. Heyman and F. A. Leckie, eds., Cambridge University Press, Cambridge, U.K., 535–609.
- Sandler, I. S., DiMaggio, F. L., and Baladi, G. Y. (1976). "Generalized cap model for geological materials." *J. Geotech. Eng. Div., Am. Soc. Civ. Eng.*, 102(7), 683–699.
- Schofield, A. N., and Wroth, C. P. (1968). *Critical state soil mechanics*, McGraw-Hill, London.
- Sekiguchi, H., and Ohta, H. (1977). "Induced anisotropy and time dependency in clays." *Constitutive equations of soils, Proc., 9th Int. Conf. on Soil Mechanics and Foundation Engineering*, Tokyo, 229–238.
- Stipho, A. S. A. (1978). "Experimental and theoretical investigation of the behavior of anisotropically consolidated kaolin." PhD thesis, Univ. College, Cardiff, U.K.
- Whittle, A. J. (1993). "Evaluation of a constitutive model for overconsolidated clays." *Geotechnique*, 43(2), 289–313.
- Whittle, A. J., and Kavvadas, M. J. (1994). "Formulation of MIT-E3 constitutive model for overconsolidated clays." *J. Geotech. Eng.*, 120(1), 173–198.